Research Article | Vol. 13, No. 3 / 1 Mar 2022 / Biomedical Optics Express 1447
Biomedical Optics EXPRESS

Femtosecond laser oocyte enucleation as a low-invasive and effective method of recipient cytoplast preparation

ALINA A. OSYCHENKO,[1,*] ALEXANDR D. ZALESSKY,[1] ULIANA A. TOCHILO,[1] DAVID YU. MARTIROSYAN,[1] YULIA YU. SILAEVA,[2] AND VICTOR A. NADTOCHENKO[1]

[1]*N.N. Semenov Federal Research Center for Chemical Physics Russian Academy of Sciences. 4 Kosygina Street, Building 1, 119991 Moscow, Russia*
[2]*Institute of Gene Biology Russian Academy of Sciences. 34/5 Vavilova Street, 119334 Moscow, Russia*
[*]*alina.chemphys@gmail.com*

Abstract: Recipient cytoplast preparation, commonly performed by DNA aspiration with a needle, inevitably leads to the loss of reprogramming factors. As an alternative to the traditional enucleation technique, femtosecond laser enucleation can eliminate DNA effectively without loss of reprogramming factors and without oocyte puncturing. In this work we have performed oocyte enucleation by destructing the metaphase plate using a 795 nm femtosecond laser. The disability of the enucleated oocytes to develop after the parthenogenetic activation, as well as the lack of DNA staining luminescence, strongly confirms the efficiency of the femtosecond laser enucleation. The parthenogenetic development of oocytes after the cytoplasm treatment suggests a low-invasive effect of the laser enucleation technique.

1. Introduction

Scientific, medical, and agricultural practice currently requires non-invasive manipulations with embryos and oocytes of animals and humans. Enucleation (removing the nucleus) and introduction of a donor nucleus are the basis of somatic cell nuclear transfer (SCNT) in animals and mitochondrial replacement therapy (MRT) in humans.

Somatic cell nuclear transfer is a widely used technology for the production of cloned animals. SCNT was firstly carried out in 1986 on sheep [1] and then repeated on several species, including mice [2,3], cattle [4], rat [5,6], rabbit [7], pig [8] and goat [9]. Despite the fact that cloning technology in mammals has existed for at least 35 years, its efficiency remains low and does not exceed several percentages (percentage of live offspring from reconstructed eggs amount).

Mitochondrial replacement therapy is relatively new. The first baby produced by MRT was born in Mexico in 2016 [10]. MRT is implemented to avoid pathologies associated with mutations in mitochondrial DNA. MtDNA mutations can lead to the misfunctioning of mitochondria and can impair the Krebs cycle, the respiratory chain, and beta-oxidation processes [11]. Such abnormalities can result in system diseases of varying severity, for example, Barth's syndrome, Pearson's syndrome, MELEAS syndrome, etc. [12].

SCNT is performed in two steps: enucleation (nuclear DNA removal) and nuclei transfer [2]. MRT can be performed in three different ways: pronuclear transfer (PNT), spindle transfer (ST) and polar body transfer (PBT) [11]. Both SCNT and ST require recipient cytoplast preparation which is commonly carried out through the aspiration of the metaphase plate within a small amount of the surrounding cytoplasm. This portion of cytoplasm contains factors responsible for nuclear remodeling and reprogramming after embryo reconstruction [13]. Maturation promoting factor (MPF) composed of two subunits ($p34^{cdc2}$ and cyclin B1) seems to be the key factor of oocyte maturation and nuclei remodeling [14,15]. Colocalization of MPF with chromosomes [16],

#449523 https://doi.org/10.1364/BOE.449523
Journal © 2022 Received 29 Nov 2021; revised 2 Feb 2022; accepted 3 Feb 2022; published 14 Feb 2022

Biomedical Optics EXPRESS

as well as some other factors essential for nuclei reprogramming [17,18], has been demonstrated. The loss of reprogramming factors via cytoplasm aspiration can be a crucial aspect of low SCNT efficiency and may affect the result of MRT.

In this research we propose to develop the method of recipient cytoplast preparation by a near-infrared femtosecond laser without aspiration of oocyte cytoplasm. Lasers are known to be the highly-precise tools which can be applied for many purposes, including SCNT. Unlike enucleation with a micropipette, laser enucleation does not imply the cell puncture and cytoplasm loss, acting locally in a strictly defined area containing DNA. Shakhbazyan et al. demonstrated the laser application for recipient cytoplast preparation [19] and for nuclei transfer which was carried out by the cell fusion [20]. Another research established the enucleation of porcine oocytes using 800 nm femtosecond (fs) laser pulses [21] with high efficiency, confirmed by the lack of parthenogenetic development of the enucleated oocytes. Enucleation with 800 nm picosecond laser is also possible [22]. Hence, the influence of the laser impact on the oocyte viability has not been estimated. To clarify this, our research included a special control group of the oocytes which were irradiated similarly to the enucleated ones but without affecting the metaphase plate. Thus, the main goal of the current work was to develop a femtosecond laser surgery method for oocyte enucleation by eliminating the metaphase plate and to test the oocyte viability after laser treatment.

The mechanisms underlying femtosecond laser nanosurgery of cells and biological tissues can be explained by chemical, thermal, and thermomechanical effects arising from low-density plasma formation under femtosecond irradiance [23–25]. The process of plasma formation mostly consists of quasi-free electron formation through the interplay of photoionization and avalanche ionization [26,27]. In terms of the oocyte metabolism and viability, the process of reactive oxygen species (ROS) generation caused by femtosecond laser pulses should be considered. Our results have shown an increase in the relative fluorescence level after laser exposure, however, no significant differences have been found with the control group.

We assume that femtosecond laser enucleation could be a safe and efficient method of recipient cytoplast preparation both for somatic cell nuclear transfer and mitochondrial replacement therapy.

2. Materials and methods

2.1. Animals and oocyte collection

The study was carried out on C57BL6/CBA female mice aged 6-8 weeks (Mus musculus). The mice were induced to superovulate by the standard method of intraperitoneal (i.p.) injection of 10 IU pregnant mare's serum gonadotropin (A036A02, Intervet) followed by an i.p. injection of 10 IU human chorionic gonadotropin (hCG) (A038A01, Intervet) 48 h later. The mice were sacrificed by cervical dislocation 17 h after hCG injection. The oviducts were placed onto a Petri dish in a drop of M2 culture medium (M7167, Sigma-Aldrich) supplemented with 0.1% hyaluronidase (H4272, Sigma-Aldrich). The ampulla of the oviduct was disrupted with a pair of thin tweezers. The oocytes purified from cumulus were placed in M2 medium in four-well dishes (179830, Nunc). We used metaphase II oocytes in the experiments.

The animal experiments were in compliance with the U.K. Animals (Scientific Procedures) Act, 1986 and were approved by the Ethics Committee of the N.N. Semenov Federal Research Center for Chemical Physics Russian Academy of Sciences.

2.2. Recipient cytoplast preparation using a femtosecond laser

To localize the metaphase plate, the oocytes were cultured in M2 medium supplemented with 5 µg/ml Hoechst 33342 dye (B2261, Sigma-Aldrich) for 15 minutes and then washed twice in M2. Visualization of the metaphase plate was performed by the lab-designed fluorescent microscope

Biomedical Optics EXPRESS

(modified IX71, Olympus) with conventional widefield UV fluorescent illumination (HBO 100, Carl Zeiss) with an additional mechanical shutter (SH05, Thorlabs) for exposure control. In all experiments UV exposure was set to 10 ms.

The metaphase plate destruction was achieved by femtosecond laser pulses. A femtosecond laser source (Mai-Tai, Spectra-Physics) was coupled to the lab-designed fluorescent microscope (modified IX71, Olympus). Femtosecond laser radiation with a wavelength of 795 nm was utilized in the following modes: trains of pulses with 100 fs duration, 80 MHz repetition rate, 0.5 nJ pulse energy (40 mW power) and 12.5 ns between pulses, total duration of the pulse trains was 60 ms. Laser radiation was focused by 60× objective lens (NA = 0.7) (LUCPlanFLN, Olympus). The laser beam waist w_0 can be calculated by the formula $0.61 \cdot \lambda / NA$. For the $\lambda = 795$ nm and NA = 0.7 the laser beam waist $w_0 = 0.7$ μm. The setup scheme was described in detail by A.D. Zalessky et al. [28,29]. The observation and imaging was performed by a XIMEA xiQ MQ013MG-ON (Ximea GmbH) or by XIMEA xiD MD061CU-SY camera (Ximea GmbH), mounted on the microscope. The oocytes were mounted in 50 μl drop of M2 medium on a coverslip (Heinz Herenz) which was placed onto a microscope stage.

Oocyte enucleation comprised several steps. At first, we visualized the metaphase plate as described above. The femtosecond laser pulses were applied in the area of the metaphase plate, and fluorescence was observed in the focal spot with each pulse simultaneously. An average size of fluorescent spot is 2.8 ± 0.8 μm. The focal length of microscope objective for visible light and for near infrared laser is slightly different. For this reason fluorescence exited by laser is slightly out of focus. Laser exposure on the metaphase plate was repeated multiple times (at average 400-500 pulse trains per oocyte) until the DNA luminescence stopped. Then the metaphase plate was visualized again. If some DNA fragments still appeared, those regions were exposed to laser action again. During the entire enucleation process, the oocytes were subjected to UV radiation no more than 5 times, hence, the total UV exposure time was 50 ms or even less. Visualization 1 contains a video demonstration of oocyte enucleation.

2.3. Oocyte parthenogenetic activation and cultivation

The oocytes were induced for haploid parthenogenetic development by 6 hours of incubation in KSOM (MR-121-D, EmbryoMax), supplemented with 5 mM strontium chloride (439665, Sigma-Aldrich) and 2 mM EGTA (E3889, Sigma-Aldrich) in CO_2-incubator with 5% CO_2 and 37°C, as described by S. Kishigami and T. Wakayama [30]. Then the oocytes were washed and cultivated overnight in KSOM in CO_2-incubator. Oocytes were observed after 6 and 24 hours of incubation to assess the development. Laser-treated and control groups were cultured in 4-well dishes (Nunc) in separate wells.

2.4. Parthenogenetic development: the experimental groups

For the experiments all oocytes were divided into 5 groups in order to distinguish the effects of laser irradiation from the other effects. The «metaphase» group (n = 106) included enucleated oocytes (enucleation is described in Sec. 2.2). In the «cytoplasm» group (n = 113), the oocytes experienced the same impact as the «metaphase» oocytes: UV illumination after the Hoechst 33342 staining was followed by the femtosecond laser exposure, but fs laser radiation was focused at any place of the cytoplasm outside the metaphase plate. An average number of pulse trains for the cytoplasm irradiation was the same as for the enucleation (400-500). Two control groups did not experience any impact (neither Hoechst staining and UV exposure nor laser exposure): the «control» oocytes (n = 105) were placed in CO_2 incubator and activated immediately after oocyte recovery, the «control + time» oocytes (n = 109) were activated together with the «metaphase» and «cytoplasm» oocytes – approximately 3 hours after the oocyte recovery (all this time «control + time», «metaphase» and «cytoplasm» oocytes were kept in M2 medium

Biomedical Optics EXPRESS

outside CO_2 incubator). And one more group was «spontaneous activation»: those oocytes were not activated by strontium.

2.5. Fluorescent dye staining and visualization

Fluorescence imaging was performed using a laser scanning confocal microscope Zeiss LSM 980 (Carl Zeiss Microscopy, Jena, Germany), 20x Plan-Apochromat objective (NA = 0.8). The oocytes were placed in M2 medium drop on a 0.17 mm cover glass (Zeiss).

2.5.1. Hoechst 33342

The oocytes were stained with 5 µg/ml Hoechst 33342 dye (B2261, Sigma-Aldrich) for 15 minutes in M2 medium and then washed twice. One-photon excitation was performed with a 405 nm laser. Fluorescence was recorded at 413-500 nm range.

2.5.2. BioTracker NIR694

The oocytes were cultured in M2 medium supplemented with BioTracker NIR694 (SCT117, Sigma-Aldrich) diluted 1:200 for 10 minutes and washed twice in M2. One-photon excitation was performed with a 639 nm laser. Fluorescence was recorded at 645-720 nm.

2.5.3. H_2DCFDA

The cell-permeant 2',7'-dichlorodihydrofluorescein diacetate (D399, Molecular probes) (H_2DCFDA) was applied as an indicator of reactive oxygen species (ROS) in the oocytes. The stock solution (1 mM H_2DCFDA in DMSO) was diluted to the working concentration of 10 µM in M2 medium. The oocytes were stained in H_2DCFDA for 15 minutes and washed in M2 for 60 minutes. Washing was necessary to avoid the drawbacks of fluorescent dye such as excessive fluorescence and buildup of fluorescence intensity. The luminescence intensity of ROS indicator was measured before and after laser exposure in the «metaphase» and «cytoplasm» oocytes. To make positive control, 0.1 mM H_2O_2 was supplemented to the oocytes. The negative control oocytes were simply visualized twice to estimate the level of fluorescence intensity buildup. One-photon excitation was performed with a 488 nm laser. Fluorescence was recorded at 492-558 nm range. Initial and final intensity mean value of H_2DCFDA luminescence was measured with ZEN 3.2 Blue Edition program for each oocyte. The intensity mean value represents an average of all intensities within the region of interest. For the interpretation, we calculated the relative fluorescence increase dividing final intensity by intensity before the laser impact or H_2O_2 addition.

3. Results

3.1. Conditions and efficiency of enucleation

In the preliminary experiments we carried out enucleation with a pulse energy of 1 nJ and pulse train duration of 30 ms. Under these settings a vapor-gas bubble appeared immediately and disrupted the cell plasma membrane, which resulted in the destruction of the oocyte. Therefore, we decreased the laser impact down to 1 nJ 15 ms and 0.5 nJ 60 ms. While 1 nJ 15 ms still induced the vapor-gas bubble, pulse energy of 0.5 nJ and pulse train duration of 60 ms appeared to be optimal parameters for the enucleation. These parameters allowed us to avoid vapor-gas bubbles but provided efficient DNA breakdown. The steps of enucleation are shown in Fig. 1. The whole metaphase plate, which is clearly visible in step A, is partly destroyed in step B and is completely absent in step C (Fig. 1). The enucleated oocytes were subsequently stained with BioTracker NIR694 to except photobleaching. The double staining revealed the lack of the metaphase plate in the enucleated oocytes, proving that DNA was actually destroyed (Fig. 2(A), (B)).

Biomedical Optics EXPRESS

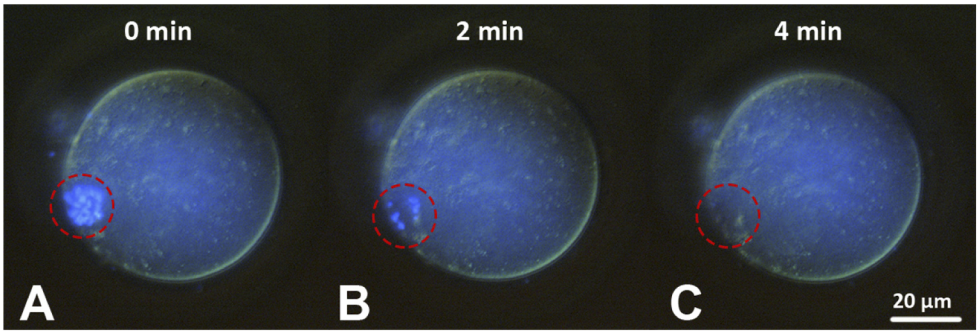

Fig. 1. Enucleation of metaphase II oocytes: A – before enucleation, B – partly destructed DNA, C – enucleated oocyte (for more details see Visualization 1).

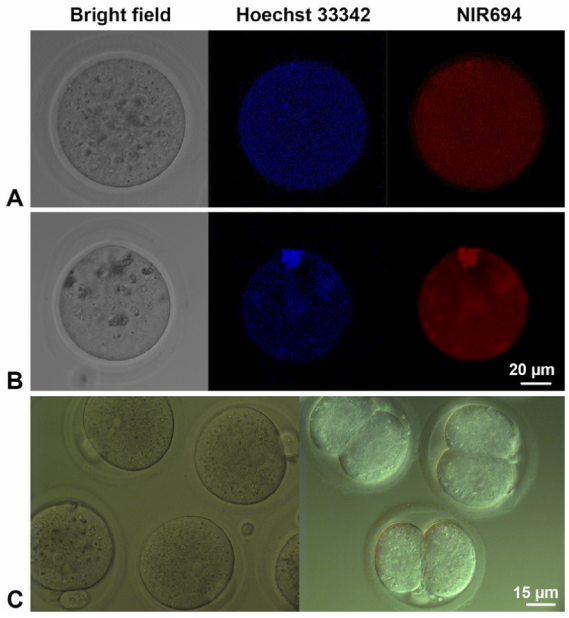

Fig. 2. Enucleated (A) and control (B) oocytes stained with Hoechst 33342 and BioTracker NIR694. (C) – development of the oocytes activated parthenogenetically. Left – the oocytes with a polar body and pronucleus, right – two-cell embryos.

3.2. Development after the laser impact

The laser-exposed and control oocytes were induced for parthenogenetic development to assess the efficiency of enucleation and the effect of laser irradiation. Most oocytes retained their viability and began to develop 6 hours after the start of parthenogenetic activation. The living and developing oocytes extruded the second polar body and some of them formed a pronucleus (Fig. 2(C), left): 89% (93/105) in the «control» group, 86% (94/109) in the «control + time», 82% (93/113) in the «cytoplasm», 6% (7/106) in the «metaphase» and 4% (4/104) in the «spontaneous activation». Some oocytes underwent fragmentation and the others had no detectable morphological changes (Table 1).

After 24 hours of parthenogenetic activation, the «cytoplasm», «control» and «control + time» oocytes formed two-cell embryos (Fig. 2(C), right) with the same efficiency: 90% (102/113),

Biomedical Optics EXPRESS

Table 1. Development of the oocytes after the haploid parthenogenetic activation.

Group	6 hours	24 hours	72 hours	96 hours
«control»	polar bodies and pronuclei 89% (93/105) no changes 9% (10/105) fragmentation 2% (2/105)	two-cell embryos 92% (97/105) no changes 0% (0/105) fragmentation 8% (8/105)	morulae 11% (12/105)	blastocysts 5% (5/105)
«control + time»	polar bodies and pronuclei 86% (94/109) no changes 14% (15/109) fragmentation 0% (0/109)	two-cell embryos 89% (97/109) no changes 7% (8/109) fragmentation 4% (5/109)	morulae 8% (9/109)	blastocysts 1% (1/109)
«cytoplasm»	polar bodies and pronuclei 82% (93/113) no changes 18% (20/113) fragmentation 0% (0/113)	two-cell embryos 90% (102/113) no changes 7% (8/113) fragmentation 3% (3/113)	morulae 11% (12/113)	blastocysts 2% (2/113)
«metaphase»	polar bodies and pronuclei 6% (7/106) no changes 90% (95/106) fragmentation 4% (4/106)	two-cell embryos 1% (1/106) no changes 15% (16/106) fragmentation 84% (89/106)	-	-
«spontaneous activation»	polar bodies and pronuclei 4% (4/104) no changes 86% (90/104) fragmentation 10% (10/104)	two-cell embryos 5% (5/104) no changes 79% (82/104) fragmentation 16% (17/104)	-	-

92% (97/105) and 89% (97/109) respectively. Some of these oocytes were capable of further development and reached the morulae and blastocyst stage. Developmental capability of the enucleated oocytes («metaphase» group) was substantially different. Though 6% of the enucleated oocytes (7/106) formed a polar body (but they did not form a pronucleus), only 1% (1/106) reached the two-cell stage. This is similar to «spontaneous activation» development: only 5% (5/104) of the oocytes were able to form two-cell embryos (Table 1).

3.3. Reactive oxygen species formation after the laser impact

H_2DCFDA was applied as an indicator for reactive oxygen species in additional series of experiments. H_2DCFDA staining revealed no significant differences in fluorescence increase between the negative control and laser-exposed oocytes (Fig. 3(A)): one-way independent ANOVA test, $p = 0.71$ for the «cytoplasm» group and $p = 0.17$ for the «metaphase» one (the description of groups is presented in Section 2.5.3), as well as between the «cytoplasm» and «metaphase» ($p = 0.74$). Positive control was significantly different from all other groups (negative control $p = 0.00001$; «cytoplasm» $p = 0.00001$; «metaphase» $p = 0.00013$).

Biomedical Optics EXPRESS

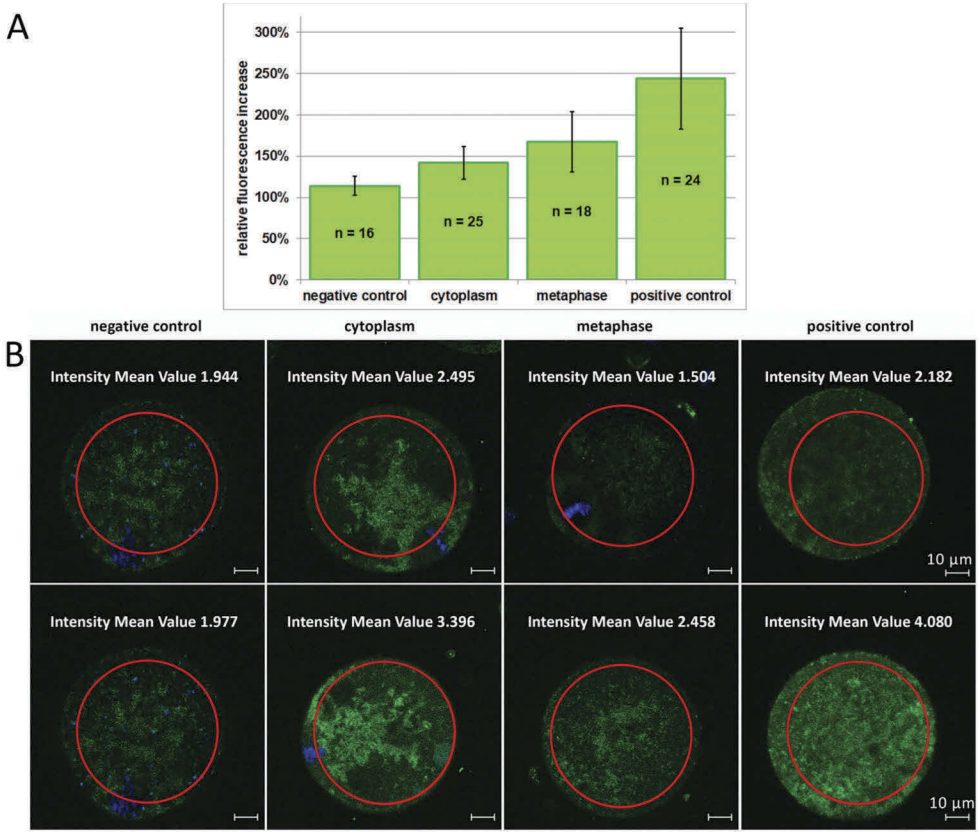

Fig. 3. A - the relative fluorescence increase of H_2DCFDA in the oocytes. The bar levels represent the mean ± standard deviation. The number of samples (n) is shown within bars. B – fluorescent images of the oocytes, stained with H_2DCFDA. Upper images are oocyte images before the experimental treatment. Lower images are the same oocytes after the laser impact or H_2O_2 supplementation. Intensity mean value represents the average of all intensities within the region of interest (the red circle). The region of interest diameter was the same for all measurements.

4. Discussion

In these experiments the main goal was to perform DNA destruction without impairment of cell integrity and viability. The intensity of the laser impact is mainly characterized by the power density calculated by division of a pulse energy (E) by the pulse duration (τ) and the area of laser beam waist (S): E / τ·S. Oocyte viability was estimated by parthenogenetic activation of the oocytes and their development rate. An additional criterion of viability was the level of reactive oxygen species.

In this work we apply laser with power density $3.25 \cdot 10^{11}$ W/cm^2, which is twice lower than the threshold for the formation of a vapor-gas bubble in the cell [28]. In our previous research we established the non-invasive range of femtosecond laser impact on living cells. According to it, the power density up to $13.2 \cdot 10^{11}$ W/cm^2 (twice exceeding the vapor-gas bubble threshold) under some conditions did not significantly affect the cell viability [29]. Being an indicator of the formation of carbon dots produced by a laser from the cell material, the vapor-gas bubble should be avoided. Carbon dots switch nonlinear absorption to linear mode at the beginning of the pulse train, causing heating and boiling [31]. The longer the pulse train duration is, the

Biomedical Optics EXPRESS

bigger the vapor-gas bubble becomes. Thus, laser irradiation power densities which produce carbon dots and vapor-gas bubbles should be avoided as the latter are able to perforate plasma membrane and subsequently destroy the cell.

The ablation threshold of DNA depends on its conformation: metaphase chromosomes require higher intensities and energies for the ablation than the nucleus itself [32]. The DNA of metaphase II oocytes is tightly packed into chromosomes and localized within a small region, typically, nearly the cell membrane. In this form the DNA is invisible in the bright-field and fluorescent staining is required for its detection. Hoechst 33342 staining, which is primarily applied for DNA visualization, significantly reduced the ablation threshold. For the chromosomes, the ablation threshold is four times higher without staining than with Hoechst staining: $4{\cdot}10^{12}$ W/cm^2 vs $1{\cdot}10^{12}$ W/cm^2 [33]. Acting as a photosensitizer, the dye helped to localize the laser impact within the area of the stained metaphase plate.

Under the 0.5 nJ and 60 ms conditions, we performed the metaphase plate ablation with high accuracy and efficiency. Staining with BioTracker NIR694, in contrast to Hoechst 33342, revealed the lack of DNA after irradiation of the metaphase plate. The enucleated oocytes were incapable of parthenogenetic activation and development. Both these facts confirm an efficient DNA breakdown. However, the laser radiation by itself seems to be low invasive. The oocytes irradiated without affecting their metaphase plate had the same rate of development as the control oocytes (90% and 92% respectively). Some of those oocytes were able to form morulae or even blastocyst, but we assumed a 2-cell stage as an indicator of a successful development because we applied haploid parthenogenetic activation.

With the femtosecond laser power density of 10^{11-14} W/cm^2 the dominant mechanisms of a low-density plasma generation are multiphoton ionization or multiphoton dissociation [25]. Free electrons of low-density plasma initiate water dissociation with the formation of hydrogen ions: H_2O^+ and H_3O^+. Excited water molecules are able to dissociate into radicals H· and OH·. Subsequently, superoxide O_2^- and singlet oxygen $^1O_2$ can be formed. Recombination of hydroxyl radicals with each other causes the formation of hydrogen peroxide H_2O_2 [34]. We used 2',7'-dichlorodihydrofluorescein diacetate as an indicator of reactive oxygen species. This method did not allow us to reveal an exact concentration of ROS, however, it enabled us to compare the ROS level between the irradiated and non-irradiated oocytes. According to the manual (Molecular probes), the dye is prone to photo-oxidation, therefore, an average of 15% fluorescence intensity buildup is due to repeated illumination. An average increase of H_2DCFDA fluorescence intensity was 70% after the enucleation and 40% after cytoplasm irradiation. It seems to be considerable, however, the significant statistical difference between laser-exposed and negative control oocytes was not found. Much higher increase (250% at average) was obtained in HeLa cells under comparable laser exposure condition, though, even this increase was below the threshold of a global ROS rise in a whole cell. Driven by the Ca^{2+}-release, ROS generation under low laser power occurred primarily in mitochondria, not in the cytosol. Mitochondrial ROS production is moderate for the cell and does not break the balance between photodamage and cellular repair system [35]. Nevertheless, much more dramatic events were observed in PtK2 cells under significantly lower laser power, applied for the confocal microscopy. The power exceeding 7 mW was enough to damage the cell membrane, induce oxidative stress and apoptosis-like cell death [36]. We did not observe any noticeable morphological changes in enucleated oocytes at least for 6 hours (Table 1). Thereby we suppose that femtosecond laser enucleation could be an appropriate method for the recipient cytoplast preparation.

5. Conclusion

In this work we developed a low-invasive method of recipient cytoplast preparation using a femtosecond laser. Tightly-focused near-infrared laser radiation does not disturb the cell integrity

Biomedical Optics EXPRESS

and viability. Thus, this method can be applied for somatic cell nuclear transfer and mitochondrial replacement therapy.

Funding. Russian Science Foundation (under grant № 21-75-10155).

Acknowledgments. This work is supported by the Russian Science Foundation under grant № 21-75-10155. The work was performed on the facilities of ACBS Center of the Collective Equipment (№ 506694, FRCCP RAS) and large-scale research facilities № 1440743. Oocyte cultivation was carried out using the unique scientific facility Transgenebank.

Disclosures. The authors declare no conflicts of interest.

Data availability. Data underlying the results presented in this paper are not publicly available at this time but may be obtained from the authors upon reasonable request.

References

1. S. M. Willadsen, "Nuclear transplantation in sheep embryos," Nature **320**(6057), 63–65 (1986).
2. L. M. Chailakhyan, B. N. Veprintsev, T. A. Sviridova, and V. A. Nikitin VA, "Electrostimulated cell fusion in cell engineering," Biofizika **32**(5), 874–887 (1987).
3. T. Wakayama, A. C. Perry, M. Zuccotti, K. R. Johnson, and R. Yanagimachi, "Full-term development of mice from enucleated oocytes injected with cumulus cell nuclei," Nature **394**(6691), 369–374 (1998).
4. J. B. Cibelli, S. L. Stice, P. J. Golueke, J. J. Kane, J. Jerry, C. Blackwell, F. A. Ponce de León, and J. M. Robl, "Cloned transgenic calves produced from nonquiescent fetal fibroblasts," Science **280**(5367), 1256–1258 (1998).
5. E. Popova, M. Bader, and A. Krivokharchenko, "Efficient production of nuclear transferred rat embryos by modified methods of reconstruction," Mol. Reprod. Dev. **76**(2), 208–216 (2009).
6. E. Popova, M. Bader, and A. Krivokharchenko, "Full-term development of rat after transfer of nuclei from two-cell stage embryos," Biol. Reprod. **75**(4), 524–530 (2006).
7. P. Chesné, P. G. Adenot, C. Viglietta, M. Baratte, L. Boulanger, and J. P. Renard, "Cloned rabbits produced by nuclear transfer from adult somatic cells," Nat. Biotechnol. **20**(4), 366–369 (2002).
8. I. A. Polejaeva, S. H. Chen, T. D. Vaught, R. L. Page, J. Mullins, S. Ball, Y. Dai, J. Boone, S. Walker, D. L. Ayares, A. Colman, and K. H. Campbell, "Cloned pigs produced by nuclear transfer from adult somatic cells," Nature **407**(6800), 86–90 (2000).
9. A. Baguisi, E. Behboodi, D. T. Melican, J. S. Pollock, M. M. Destrempes, C. Cammuso, J. L. Williams, S. D. Nims, C. A. Porter, P. Midura, M. J. Palacios, S. L. Ayres, R. S. Denniston, M. L. Hayes, C. A. Ziomek, H. M. Meade, R. A. Godke, W. G. Gavin, E. W. Overström, and Y. Echelard Y, "Production of goats by somatic cell nuclear transfer," Nat. Biotechnol. **17**(5), 456–461 (1999).
10. J. Zhang, G. Zhuang, Y. Zeng, J. Grifo, C. Acosta, Y. Shu, and H. Liu, "Pregnancy derived from human zygote pronuclear transfer in a patient who had arrested embryos after IVF," Reprod. BioMed. Online **33**(4), 529–533 (2016).
11. D. P. Wolf, N. Mitalipov, and S. Mitalipov, "Mitochondrial replacement therapy in reproductive medicine," Trends Mol. Med. **21**(2), 68–76 (2015).
12. A. M. Schaefer, R. W. Taylor, D. M. Turnbull, and P. F. Chinnery, "The epidemiology of mitochondrial disorders—past, present and future," Biochim. Biophys. Acta, Bioenerg. **1659**(2-3), 115–120 (2004).
13. K. H. Campbell, "Nuclear transfer in farm animal species," Semin. Cell Dev. Biol. **10**(3), 245–252 (1999).
14. N. Hashimoto and T. Kishimoto, "Cell cycle dynamics of maturation-promoting factor during mouse oocyte maturation," Tokai J. Exp. Clin. Med. **11**(6), 471–477 (1986).
15. J. Gautier, J. Minshull, M. Lohka, M. Glotzer, T. Hunt, and J. L. Maller, "Cyclin is a component of maturation-promoting factor from Xenopus," Cell **60**(3), 487–494 (1990).
16. L. J. Huo, L. Z. Yu, C. G. Liang, H. Y. Fan, D. Y. Chen, and Q. Y. Sun, "Cell-cycle-dependent subcellular localization of cyclin B1, phosphorylated cyclin B1 and p34cdc2 during oocyte meiotic maturation and fertilization in mouse," Zygote **13**(1), 45–53 (2005).
17. Y. B. Luo, L. Zhang, Z. L. Lin, J. Y. Ma, J. Jia, S. Namgoong, and Q. Y. Sun, "Distinct subcellular localization and potential role of LINE1-ORF1P in meiotic oocytes," Histochem. Cell Biol. **145**(1), 93–104 (2016).
18. C. J. Huang, Y. F. Yuan, D. Wu, F. A. Khan, X. F. Jiao, and L. J. Huo, "The cohesion stabilizer sororin favors DNA repair and chromosome segregation during mouse oocyte meiosis," In Vitro Cell. Dev. Biol.: Anim. **53**(3), 258–264 (2017).
19. A. K. Shakhbazyan, T. A. Sviridova-Chailakhyan, A. K. Karmenyan, A. S. Krivokharchenko, A. Chiou, and L. M. Chailakhyan, "The use of laser for obtaining recipient cytoplasts for mammalian nuclear transfer," Dokl. Biol. Sci. **428**(1), 475–478 (2009).
20. A. K. Shakhbazyan, T. A. Sviridova-Chailakhyan, A. K. Karmenyan, A. S. Krivokharchenko, A. Chiou, and L. M. Chailakhyan, "The possibilities of optical laser technologies in cell engineering," Dokl. Biol. Sci. **429**(1), 587–590 (2009).
21. K. Kuetemeyer, A. Lucas-Hahn, B. Petersen, E. Lemme, P. Hassel, H. Niemann, and A. Heisterkamp, "Combined multiphoton imaging and automated functional enucleation of porcine oocytes using femtosecond laser pulses," J. Biomed. Opt. **15**(4), 046006 (2010).

Biomedical Optics EXPRESS

22. A. V. Karmenyan, A. K. Shakhbazyan, T. A. Sviridova-Chailakhyan, A. S. Krivokharchenko, A. E. Chiou, and L. M. Chailakhyan, "Use of picosecond infrared laser for micromanipulation of early mammalian embryos," Mol. Reprod. Dev. **76**(10), 975–983 (2009).
23. A. Vogel, J. Noack, and G. Hüttman andG. Paltauf, "Mechanisms of femtosecond laser nanosurgery of cells and tissues," Appl. Phys. B **81**(8), 1015–1047 (2005).
24. V. Venugopalan, A. Guerra, K. Nahen, and A. Vogel, "Role of laser-induced plasma formation in pulsed cellular microsurgery and micromanipulation," Phys. Rev. Lett. **88**(7), 078103 (2002).
25. A. Vogel and V. Venugopalan, "Mechanisms of pulsed laser ablation of biological tissues," Chem. Rev. **103**(2), 577–644 (2003).
26. D. X. Hammer, R. J. Thomas, G. D. Noojin, B. A. Rockwell, P. K. Kennedy, and W. P. Roach, "Experimental investigation of ultrashort pulse laser-induced breakdown thresholds in aqueous media," IEEE J. Quantum Electron. **32**(4), 670–678 (1996).
27. A. A. Oraevsky, L. B. Da Silva, A. M. Rubenchik, M. D. Feit, M. E. Glinsky, M. D. Perry, B. M. Mammini, W. Small, and B. C. Stuart, "Plasma mediated ablation of biological tissues with nanosecond-to-femtosecond laser pulses: relative role of linear and nonlinear absorption," IEEE J. Sel. Top. Quantum Electron. **2**(4), 801–809 (1996).
28. A. D. Zalessky, A. A. Osychenko, A. N. Kostrov, A. V. Ryabova, A. S. Krivokharchenko, and V. A. Nadtochenko, "Femtosecond laser surgery of two-cell mouse embryos: effect on viability, development, and tetraploidization," J. Biomed. Opt **22**(12), 125006 (2017).
29. A. A. Osychenko, U. A. Tochilo, A. A. Astafiev, A. D. Zalessky, A. M. Shakhov, A. S. Krivokharchenko, and V. A. Nadtochenko, "Determining the range of noninvasive near-infrared femtosecond laser pulses for mammalian oocyte nanosurgery," Sovrem Tehnol. Med. **9**(1), 21–26 (2017).
30. S. Kishigami and T. Wakayama, "Efficient strontium-induced activation of mouse oocytes in standard culture media by chelating calcium," J. Reprod. Dev. **53**(6), 1207–1215 (2007).
31. A. A. Astafiev, A. M. Shakhov, A. A. Osychenko, M. S. Syrchina, A. V. Karmenyan, U. A. Tochilo, and V. A. Nadtochenko, "Probing intracellular dynamics using fluorescent carbon dots produced by femtosecond laser in situ," ACS Omega **5**, 12527 (2020).
32. A. Uchugonova, M. Lessel, S. Nietzsche, C. Zeitz, K. Jacobs, C. Lemke, and K. Koenig, "Nanosurgery of cells and chromosomes using near-infrared twelve-femtosecond laser pulses," J. Biomed. Opt. **17**(10), 101502 (2012).
33. K. Kuetemeyer, R. Rezgui, H. Lubatschowski, and A. Heisterkamp, "Influence of laser parameters and staining on femtosecond laser-based intracellular nanosurgery," Biomed. Opt. Express **1**(2), 587–597 (2010).
34. J. Baumgart, K. Kuetemeyer, W. Bintig, A. Ngezahayo, W. Ertmer, H. Lubatschowski, and A. Heisterkamp, "Repetition rate dependency of reactive oxygen species formation during femtosecond laser-based cell surgery," J. Biomed. Opt. **14**(5), 054040 (2009)..
35. W. Yan, H. He, Y. Wang, Y. Wang, M. Hu, and C. Wang, "Controllable generation of reactive oxygen species by femtosecond-laser irradiation," Appl. Phys. Lett. **104**(8), 083703 (2014).
36. U. K. Tirlapur, K. König, C. Peuckert, R. Krieg, and K.-J. Halbhuber, "Femtosecond near-infrared laser pulses elicit generation of reactive oxygen species in mammalian cells leading to apoptosis-like death," Exp. Cell Res. **263**(1), 88–97 (2001).